

Exciton formation and dissociation in mass-asymmetric electron-hole plasmas

H. Fehske¹, V. Filinov^{2,3}, M. Bonitz³, V. Fortov² and P. Levashov²

¹Institut für Physik, Ernst-Moritz-Arndt-Universität Greifswald, Domstrasse 10a, D-17489 Greifswald, Germany

²Institute for High Energy Density, Russian Academy of Sciences, Izhorasky 13/19, Moscow 127412, Russia

³Christian-Albrechts-Universität zu Kiel, Institut für Theoretische Physik und Astrophysik, Lehrstuhl Statistische Physik, Leibnizstrasse 15, 24098 Kiel, Germany

Abstract. First-principle path integral Monte Carlo simulations were performed in order to analyze correlation effects in complex electron-hole plasmas, particularly with regard to the appearance of excitonic bound states. Results are discussed in relation to exciton formation in unconventional semiconductors with large electron hole mass asymmetry.

1. Introduction

Strongly coupled Coulomb systems have been in the focus of recent investigations in many fields, including plasma, nuclear, condensed matter and astrophysics [1, 2, 3, 4]. In these systems the Coulomb energy is of the order of, or even exceeds the mean kinetic energy. Besides, quantum effects are of vital importance. The formation of Coulomb liquids and solids is only one of the multi-faceted phenomena that might show up. Just now the existence of Coulomb crystals has been studied for neutral plasmas containing (at least) two oppositely charged components [5]. Most notably crystallization of holes in semiconductors was predicted to occur in materials with a sufficiently large hole to electron effective mass asymmetry of about 80.

Since bound state formation turned out to be the relevant limiting factor for the appearance of such an exceptional quantum hole (Coulomb) crystal at low temperatures [5], the aim of the present contribution is to analyze the formation of excitons in mass asymmetric electron-hole plasmas from first principles. A theoretical approach that is well suited to address this problem is the direct path integral quantum Monte Carlo (DPIMC) method for the N-particle density operator [6]. The DPIMC technique avoids additional approximations, such as the fixed node and restricted path integral method. It has been successfully applied to treat both strong interaction and quantum effects [6, 7, 8].

The organization of the paper is as follows. In Sec. 2 we briefly describe the essence of the DPIMC method we employed. Section 3 presents our simulation results. There we will give a detailed discussion of typical many-particle configurations at low and high temperatures, as well as of electron-electron, hole-hole and electron-hole pair distribution functions and structure factors. We conclude in Sec. 3, relating our results to the heavily debated exciton formation in intermediate valent Tm[Se,Te] [9].

2. Direct path integral Monte Carlo approach

The starting point for the description of a two-component (equilibrium) quantum plasma is the partition function given at inverse temperature $\beta = 1/k_B T$ by

$$Z(N_e, N_h, V, \beta) = \frac{1}{N_e! N_h!} \sum_{\sigma} \int_V dq \rho(q, \sigma; \beta), \quad (1)$$

where $q = \{q_e, q_h\}$ and $\sigma = \{\sigma_e, \sigma_h\}$ denote the spatial coordinates and spin degrees of freedom of N_e electrons and N_h holes ($N_e = N_h$), respectively, i.e. $q_a = \{q_{1,a} \dots q_{l,a} \dots q_{N_a,a}\}$ and $\sigma_a = \{\sigma_{1,a} \dots \sigma_{l,a} \dots \sigma_{N_a,a}\}$ with $a = e, h$. Then the pair distribution functions and the charge structure factors can be expressed as [10]

$$g_{ab}(r) = \frac{N_e! N_h!}{Z(N_e, N_h, \beta)} \sum_{\sigma} \int_V dq \delta(r_{1,a} - q_{1,a}) \delta(r_{2,b} - q_{2,b}) \rho(q, \sigma; \beta) \quad (2)$$

and

$$S_{ab}(k) = \frac{\int_0^\infty dr r^2 [g_{ab}(r) - 1] \sin(kr)/(kr)}{|\int_0^\infty dr r^2 (g_{ab}(r) - 1)|}, \quad (3)$$

where $r = r_{1,a} - r_{2,b}$.

Of course, in general the exact density matrix $\rho(q, \sigma; \beta)$ of an interacting quantum many-particle systems is not known but can be constructed using a path integral approach:

$$\begin{aligned} \int_V \sum_{\sigma} dq^{(0)} \rho(q^{(0)}, \sigma; \beta) &= \int_V dq^{(0)} \dots dq^{(n)} \rho^{(1)} \cdot \rho^{(2)} \dots \rho^{(n)} \\ &\times \sum_{\sigma} \sum_{P_e} \sum_{P_h} (\pm 1)^{\kappa_{P_e} + \kappa_{P_h}} \mathcal{S}(\sigma, \hat{P}_e \hat{P}_h \sigma'_a) \hat{P}_e \hat{P}_h \rho_{q_a^{(n+1)}=q_a^{(0)}, \sigma'_a=\sigma_a}^{(n+1)}. \end{aligned} \quad (4)$$

Here $\rho^{(i)} \equiv \rho(q^{(i-1)}, q^{(i)}; \Delta\beta) \equiv \langle q^{(i-1)} | e^{-\Delta\beta \hat{H}} | q^{(i)} \rangle$ and $\Delta\beta \equiv \beta/(n+1)$. The Hamiltonian for the electron-hole plasma ($\hat{H} = \hat{K} + \hat{U}$) contains kinetic energy (\hat{K}) and Coulomb interaction

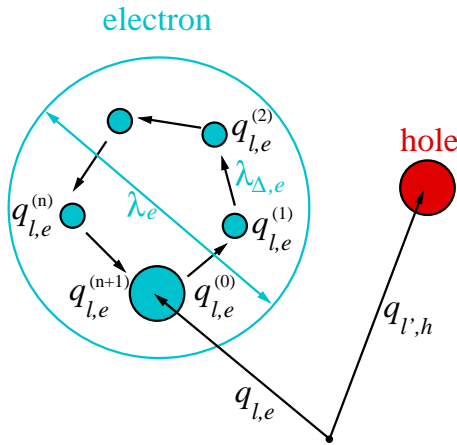


Figure 1. (Color online) Bead representation of electrons and holes. Here $\lambda_e^2 = 2\pi\hbar^2\beta/m_e$, $\lambda_{\Delta,e}^2 = 2\pi\hbar^2\Delta\beta/m_e$, $q_{l,e}^{(1)} = q_{l,e}^{(0)} + \lambda_{\Delta,e}\xi_{l,e}^{(1)}$, and $\sigma = \sigma'$. The holes have a similar beads representation, however λ_h is $\sqrt{m_e/m_h}$ times smaller.

energy ($\hat{U} = \hat{U}_{ee} + \hat{U}_{hh} + \hat{U}_{eh}$) parts. In Eq. (4) the index $i = 1 \dots n + 1$ labels the high-temperature $[(n + 1)k_B T]$ density matrices $\rho^{(i)}$. Accordingly each particle is represented by $(n + 1)$ beads, i.e. the whole configuration of the particles is represented by a $3(N_e + N_h)(n + 1)$ -dimensional vector $\tilde{q} \equiv \{q_{1,e}^{(0)}, \dots, q_{1,e}^{(n+1)}, q_{2,e}^{(0)}, \dots, q_{2,e}^{(n+1)}, \dots, q_{N_e,e}^{(0)}, \dots, q_{N_e,e}^{(n+1)}; q_{1,h}^{(0)}, \dots, q_{N_h,h}^{(n+1)}\}$. Further details of the high-temperature path integral representation are given in Ref [6].

Figure. 1 illustrates the representation of one (light) electron and one (heavy) hole. The circle around the electron beads symbolizes the region that mainly contributes to the partition function path integral. The size of this region is of the order of the thermal electron wavelength $\lambda_e(T)$, while typical distances between electron beads are of the order of the electron wavelength taken at $(n + 1)$ -times higher temperatures. The same representation is valid for holes but due to the larger hole mass the characteristic length scales are smaller by a factor of $\sqrt{m_e/m_h}$. The spin gives rise to the spin part of the density matrix (\mathcal{S}) with exchange effects accounted for by the permutation operators \hat{P}_e and \hat{P}_h acting on the electron and hole coordinates $q^{(n+1)}$ and spin projections σ' . The sum is over all permutations with parity κ_{P_e} and κ_{P_h} .

In the evaluation of the expressions obtained so far, we make use of a Monte Carlo scheme [12] with different types of Monte Carlo steps: Either electron or hole coordinates ($q_{l,a}$) or dimensionless individual electron or hole beads ($\xi_{l,a}^{(i)}$) were moved until convergence is reached. Periodic boundary conditions are applied to the basic Monte Carlo cell. The procedure has been extensively tested. For example, the comparison with the known analytical expressions for pressure and energy of an ideal Fermi gas showed that Fermi statistics is well reproduced [6]. Moreover we applied the method to few-electron systems in harmonic traps where again the analytically known limiting behavior of the energy was recovered [8]. For the present simulations of an mass-asymmetric electron-hole plasma, we have varied both particle and beads numbers and found that in order to obtain convergent results particle numbers $N_e = N_h = 50$ and beads numbers in the range of $N_b = 20$ are sufficient. Thereby the density matrix in the high temperature decomposition always was taken at temperatures above the electron-hole binding energy. Finally let us emphasize that the maximum statistical error of the results presented below is about 5% and can be systematically reduced by increasing the length of the Monte Carlo run.

3. Simulation results

We now use the DPIMC scheme outlined in the preceding section in order to study exciton formation in (non-ideal) electron-hole plasmas. Independent model parameters are the temperature (T), the masses of electrons (m_e) and holes (m_h), and the static dielectric constant (ε). The plasma density is characterized by the Brueckner parameter r_s , defined as the ratio of the mean distance between the particles $d = [3/(4\pi(n_e + n_h))]^{1/3}$ and the Bohr radius a_B [11], where n_e and n_h are electron and hole densities, respectively. To make contact with experiments on the Tm[Te,Se] system [9], we choose $m_e = 2$, $m_h = 80$, and $\varepsilon = 25$ (the masses are in units of the free electron mass). Then, assuming a simple Wannier exciton picture, the exciton binding energy would be about 500 K.

3.1. Particle configurations

Figure 2 shows typical “snapshots” of an electron-hole many-particle state with $r_s = 10$ at low (50K) and high (200K) temperatures. Here, as a result of the temperature decomposition of the density matrix, each electron and hole is represented by several beads. Since the number of beads is twenty the high temperature density matrices correspond to a temperature of at least 1000K, being about two times larger than the characteristic (excitonic) binding energy (E_X^b).

The spatial distribution of the beads reflects the position probability amplitude of the many-particle wave function, where the characteristic size of a certain cloud of beads is of the order

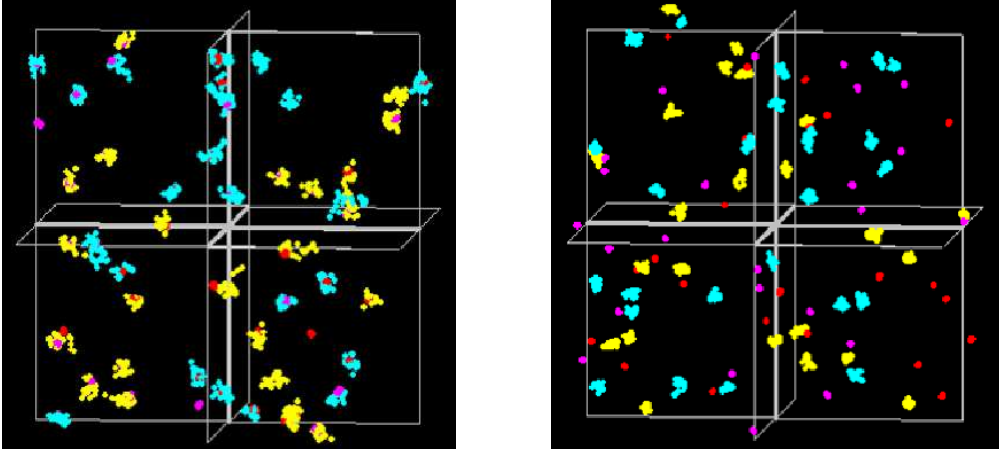


Figure 2. (Color online) Snapshots of the electron-hole plasma at $T = 50K$ (left) and $T = 200K$ (right) (for $r_s = 10$). Clouds of blue (yellow) dots represent electrons with spin up (down), whereas red (pink) dots mark the holes. Grey lines indicate the main simulation box which is periodically repeated in all spatial directions.

of the thermal wave length of a single quantum particle. Because of the mass asymmetry the typical size of the electron clouds is about 6 times larger than that of the holes. Also, increase of the temperature leads to a reduce of the particle extension. Interestingly, at low temperatures practically all holes are closely covered by electron beads. This means electrons and holes form predominantly bound states and the whole system consists mainly of excitons. From Fig. 2 we can see that the average distance between particles (unbound electrons, holes and excitons) is much larger than the size of the excitons. At higher temperatures ($T = 200K$) we observe a significant number of free electrons and holes (cf. Fig. 2, right panel). Due to the temperature-induced dissociation of the excitonic bound states a partially ionized (non-ideal) electron-hole plasma is formed.

3.2. Pair distribution functions and structure factors

This scenario is supported by the behavior of the electron-electron, hole-hole and electron-hole correlations pointed out in this section. The pair distribution functions and structure factors shown in Fig. 3 are the sum over both spin projections of the particles.

Let us first discuss the physics at short distances in terms of the pair distribution functions. The function g_{ab} is the distribution of b-particles, on the average, about any a-particle. As an effect of the Coulomb and Fermi (statistics) repulsion, g_{ee} and g_{hh} are strongly depleted at small r . The decay of the hole-hole correlations is much stronger because of the larger masses, i.e. holes behave more “classically”. For the electron subsystem quantum exchange and tunnelling are more important and compete with the Coulomb repulsion. Furthermore the pronounced peak of the electron-hole pair distribution unambiguously signals the formation exciton bound states. This is confirmed by considering the product $r^2 g_{eh}(r)$ which has the physical meaning of the probability to find the electron at distance r away from the hole. At low temperatures, $r^2 g_{eh}(r)$ is strongly peaked around a_B . Increasing the temperature the excitonic peak weakens and finally it vanishes at about 300 K, which reflects thermal dissociation of excitons. Note that g_{ee} and g_{hh} (almost) coincide even at short distances for 200 K, i.e. the now electrons behave more like “classical” particles as well. Clearly all functions g_{ab} go to unity at large distances for all T , which is a result of the overall uniform distributions of the charges.

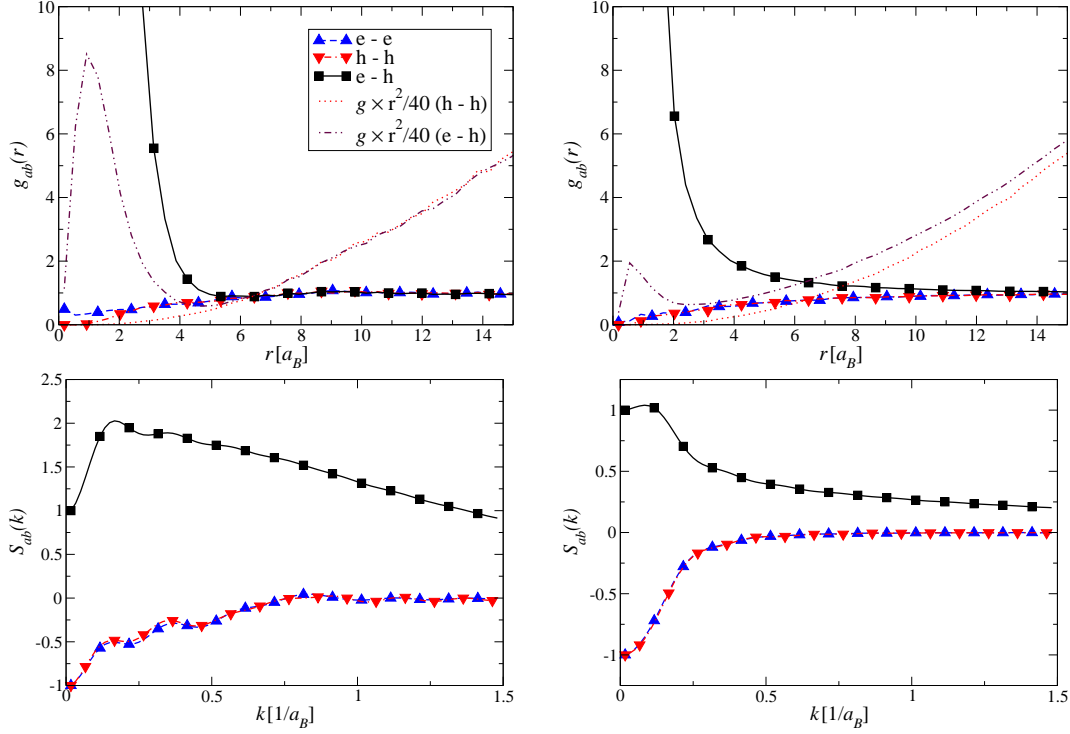


Figure 3. (Color online) Pair distribution functions (upper panels) and structure factors (lower panels) at $T = 50K$ (left panels) and $T = 200K$ (right panels), respectively. Results are given for $r_s = 10$.

To discuss the physical behavior at large distances in more detail, it is convenient to consider the (charge) structure factor S_{ab} in momentum space. According to Eq. (3) positive (negative) values of S_{ab} indicate attraction (repulsion). From g_{eh} the typical length scale of the attractive electron-hole correlations was found to be of the order of $5a_B$ at 50 K (cf., Fig. 3, upper left panel). Exciton formation sets a new length scale for the structure factor as well (cf. the maximum in the structure factor at about $0.2 [1/a_B]$). In accordance with the above discussion this excitonic maximum is shifted to smaller k values and finally washed out if the temperature is raised. In the case that the maximum (minimum) of S_{ab} is located at $k = 0$ and $S_{ab}(k)$ is a monotonically decreasing (increasing) and rather structure-less function of k ; the system closely resembles a homogeneous electron-hole plasma. Nontrivial quantum (screening) effects, however, come into play at low temperatures as can be seen from the wiggly behavior especially of the electron-electron and hole-hole charge correlations.

3.3. Exciton density

From the analysis of the snapshots in Sec. 3.1 we found that our complex electron-hole plasma contains at the same time free electrons, holes and excitons. That means, depending on the temperatures and particle densities, electrons and holes may appear in bound and unbound quantum and classical states. In a strict sense, we cannot calculate the fraction of bound and free states in our DPIMC simulations because of the possible overlapping of the electron “shells”, in particular at intermediate temperatures. Nevertheless a rough estimation of the fraction of the number of electron-hole bound states can be obtained by the following physical reasonings.

The contribution of all bound and scattering states at temperature $1/\beta$ is given by the two-

particle Slater sum

$$\Sigma_{eh}(r, \beta) = 8\pi^{3/2} \lambda_{eh}^3 \sum_{E_\alpha=E_0}^{\infty} |\Psi_\alpha(r)|^2 \exp(-\beta E_\alpha), \quad (5)$$

where E_α and $\Psi_\alpha(r)$ are the energy (without the center of mass energy) and the wave function of the exciton, respectively. Σ_{eh} is, in essence, the diagonal part of the density matrix and the product $r^2 \Sigma_{eh}$ represents the (quantum mechanical) probability for an electron and a hole to be separated by distance r .

The sum over all possible states contains contributions from the discrete (d) and continuum (c) part of the spectrum, $\Sigma_{eh} = \Sigma^d + \Sigma^c$. Σ^d contains all populated bound states between E_0 and energy E' that separates bound and free (scattering) states. For low densities it is reasonable to choose $E' \approx -\frac{3}{2\beta}$ since higher lying bound states will be thermally ionised [12].

At temperatures smaller than the electron-hole binding energy and distances smaller or of the order of several Bohr radii, the main contribution to the Slater sum comes from electron-hole bound states, while at larger distances free electron-hole scattering states turn out to be the crucial factor. We found that the product $r^2 \Sigma_{eh}$ is sharply peaked around a_B , just like $r^2 g_{eh}(r)$ in Fig. 3, where the maximum is most pronounced at low temperatures. Increasing the temperature, $r^2 g_{eh}(r)$ approaches the parabola r^2 related to the case of full absence of bound states (ideal plasma $g_{eh}(r) \equiv 1$). An attractive interaction results in an increase of the pair distribution function at short e-h distances: $g_{eh}(r) > 1$ for $0 \leq r \leq r^b$. Since the total number of particles is conserved this increase involves a decrease at large distances (see Fig. 3). So the interval $[0, r^b]$ with $r^2 * (g_{eh}(r) - 1) > 0$ gives the contribution of the bound states to the total, bound and scattering state probability. In a strict sense, correlated e-h scattering states also contribute to the maximum of $g_{eh}(r)$, but their influence is negligible for the temperatures considered, where r^b is of the order of several Bohr radii. For example, for $T = 50K$ only excitons with the principle quantum number $n = 1$ and $n = 2$ are stable, which corresponds to a predominant electron-hole separation in the range of about $4a_B$. This is well reproduced by the procedure outlined above which yields $r^b \simeq 3.7a_B$, cf. Fig. 3 (upper left part). Hence the fraction of the electron-hole bound states can be estimated from the ratio

$$\frac{N_{eh}^b}{N_{eh}^b + N_{eh}^c} = \frac{\int_0^{r^b} r^2 * [g_{eh}(r) - 1] dr}{\int_0^{r^b} r^2 * g_{eh}(r) dr}, \quad (6)$$

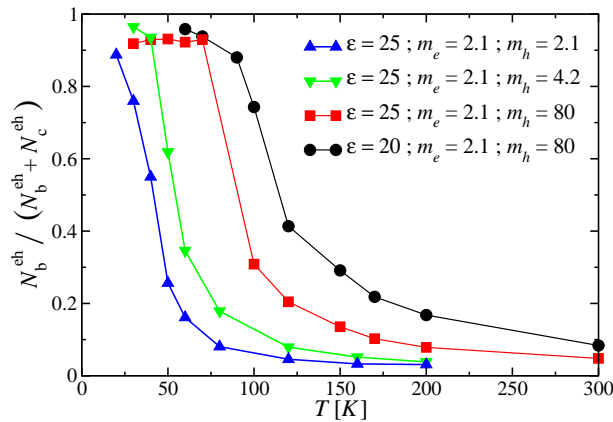


Figure 4. (Color online) Fraction of electron-hole bound states versus temperature for different hole masses and dielectric constants.

where the denominator is the normalization constant and has the physical meaning of electrons to be in bound or scattering states.

Figure 4 shows the temperature dependence of the fraction of electron-hole bound states calculated using Eq. (6) for two dielectric constants and different electron to hole mass ratios. Obviously, larger ϵ 's result in lower electron-hole binding energies and therefore shift the ionization temperature to smaller values. The same tendency is observed if m_h/m_e is lowered. For example, from Fig. 4 we found that the ratio of the temperatures, where the fraction of electron-hole bound states is 50%, is the same as the corresponding ratio of the reduced electron-hole masses $\mu = m_e m_h / (m_e + m_h)$ (keeping ϵ fixed). We have a ratio of about 2 for the data belonging to $m_h = 80$ and $m_h = 2.1$, and 1.5 for those belonging to $m_h = 80$ and $m_h = 4.2$. This is exactly what we would expect from the ideal Saha equation because the exciton binding energy is known to be proportional to the reduced electron-hole mass.

4. Conclusions

To summarize, we have performed a largely unbiased direct path integral quantum Monte Carlo simulation of a neutral non-ideal two-component Coulomb system consisting of light electrons and heavy holes. The careful analysis of typical many-particle configurations, pair distribution and charge structure functions reveals a rather comprehensive physical picture of how the system behaves as a function of temperature in the low-density regime. We obtained clear evidence for exciton formation at low temperatures and a temperature-induced dissociation of these electron-hole bound states. The ionization temperature strongly depends on the dielectric constant and the mass ratio of electrons and holes, where small values of ϵ and large mass asymmetry stabilize the bound states. As found out recently, these excitonic bound states are the limiting factor for a possible Coulomb crystallization of the heavy holes at low densities [5]. At large temperatures the system resembles an electron-hole plasma.

Electron-hole systems with such a strong mass anisotropy are realized in intermediate valent $\text{Tm}[\text{Se}_x\text{Te}_{1-x}]$ alloys [9]. In these materials f-d hybridization provides us with a narrow dispersive f valence band and, as a consequence, with a large effective hole mass of the order of 50-100 (bare) electron masses. $\text{TmSe}_{0.45}\text{Te}_{0.55}$ is, at ambient conditions, an indirect semiconductor having a gap of $E_\Delta = 130$ meV, where with $E_X^b \simeq 50 - 70$ meV below the bottom of the d band an excitonic level has been observed. Applying pressure the gap can be tuned (and even closed) and the material is speculated to realize in the pressure region between 5 and 11 kbar an excitonic insulator, the search for which has been run for a long time. A necessary precondition is the existence of a large number of (up to $\sim 10^{20}$) excitons with intermediate size (in order to avoid too strong overlap of the excitonic bound states) [9]. Surprisingly, in $\text{TmSe}_{0.45}\text{Te}_{0.55}$ the excitonic phase then is predicted to be stable at rather high temperatures (up to 200 K). Using the $\text{Tm}[\text{Se}_x\text{Te}_{1-x}]$ parameters within our (surely oversimplified) two-component Coulomb model DPIMC simulation, we could at least corroborate this belief. We found that (i) the fraction of excitonic bound states amounts to 80-90 %, (ii) the bound states will be stable up to 100-150 K, and (iii) the mass asymmetry between holes and electron is crucial therefore. As yet we are not in the position to detect the condensed excitonic phase. Feasible, however, should be the investigation of the density dependence of the various quantities. Here we expect to see the formation of bi-exciton bound states and finally the Mott transition at large particle densities n_a (i.e. small r_s). Note that the excitonic-insulator semi-metal (Mott) transition has been detected to occur in $\text{TmSe}_{0.45}\text{Te}_{0.55}$ at a pressure of about 13-14 kbar for $T \rightarrow 0$. Work along this line is in progress.

Acknowledgements

This work was supported by RF President Grant No. MK-1769.2003.08, RAS program No. 17 and Deutsche Forschungsgemeinschaft through BO 1366/2 and FE 398/6. Research was also partly sponsored by Award No. PZ-013-02 of the U.S. Civilian Research & Development Foundation for the Independent States of the Former Soviet Union (CRDF) and of Ministry of Education of Russian Federation. The authors would like to thank G. Schubert and G. Wellein for assistance by implementing the code on diverse parallel compute clusters.

References

- [1] Kalman G. et al. (Eds.) 1998, *Strongly Coupled Coulomb Systems*, Plenum Press (New York)
- [2] Bonitz M, *Quantum kinetic theory*, Teubner, Stuttgart, Leipzig 1998
- [3] *Progress in Nonequilibrium Greens functions*, M. Bonitz (ed.), World Scientific, Singapore, 2000
- [4] *Progress in Nonequilibrium Greens functions II*, M. Bonitz and D. Semkat (Eds.), World Scientific, Singapore, 2003
- [5] Bonitz M, Filinov V S, Fortov V E, Levashov P, and Fehske H, unpublished.
- [6] Filinov V S, Bonitz M, and Fortov V E 2000 JETP Letters **72**, 245; Filinov V S, Bonitz M, Ebeling W, and Fortov V E 2001, Plasma Phys. Contr. Fusion **43**, 743
- [7] Filinov V S, Fortov V E, Bonitz M, and Kremp D 2000, Phys. Lett. A **274**, 228
- [8] Filinov A V, Lozovik Y E, and Bonitz M 2000, phys. stat. sol. (b) **221**, 231; Filinov A V, Bonitz M, and Lozovik Y E 2001, Phys. Rev. Lett. **86**, 3851
- [9] Wachter P, Bucher B, and Malar J 2004, Phys. Rev. B **69**, 094502
- [10] Fisher I Z 1961, *Statistical theory of liquids*, GIFML, Moscow (in Russian)
- [11] Note that the distance between two electrons (two holes) is $d2^{1/3}$ and the conventional Bruckner parameter of electrons (holes) follows from our definition by multiplication with the $2^{1/3}$.
- [12] Zamalin V M, Norman G E, and Filinov V S 1977, *The Monte Carlo Method in Statistical Thermodynamics*, Nauka (Moscow) (in Russian)